

Mechanism of effective three-photon induced lasing

H. H. Fan, Y. J. He, J. W. Dong, B. C. Chen, H. Z. Wang, Y. P. Tian, and M. F. Reid

Citation: *Appl. Phys. Lett.* **96**, 021109 (2010); doi: 10.1063/1.3291671

View online: <http://dx.doi.org/10.1063/1.3291671>

View Table of Contents: <http://aip.scitation.org/toc/apl/96/2>

Published by the [American Institute of Physics](#)

The logo for Scilight, with 'Sci' in white and 'light' in a yellow-orange gradient.

Sharp, quick summaries **illuminating**
the latest physics research

Sign up for **FREE!**

The logo for AIP Publishing, with 'AIP' in a white box above 'Publishing' in a smaller white box.

Mechanism of effective three-photon induced lasing

H. H. Fan,¹ Y. J. He,¹ J. W. Dong,¹ B. C. Chen,¹ H. Z. Wang,^{1,a)} Y. P. Tian,² and M. F. Reid³

¹State Key Laboratory of Optoelectronic Materials and Technologies, Zhongshan (Sun Yat-Sen)

University, Guangzhou 510275, People's Republic of China

²Department of Chemistry, Anhui University, Hefei 230039, People's Republic of China

³Department of Physics and Astronomy, University of Canterbury, Christchurch 8020, New Zealand

(Received 8 September 2009; accepted 20 December 2009; published online 14 January 2010)

The experimental and theoretical results in this letter reveal that three-photon absorption effect can help light wave to form solitonlike filament; and a stable solitonlike filament is observed in solution with high quintic nonlinearity. This stable solitonlike filament makes pumping infrared laser be localized within the filament and reach high pumping density for a long distance. This high density pumping laser in the filament generates high efficiency lasing induced by three-photon absorption. This work is an approach to make practical application of high order nonlinear optical processes possible. © 2010 American Institute of Physics. [doi:10.1063/1.3291671]

Two-photon absorption processes was predicted theoretically in 1931 (Ref. 1) and observed² experimentally in 1961, but it didn't cause considerable attention until numerous applications of two-photon excitation were reported.³⁻⁷ These applications had attracted interest in exploring effective two-photon absorption materials.^{8,9} Later three-photon induced lasing was reported,^{10,11} which efficiency reached 5.4%¹¹ and is at the same order as that of two-photon induced lasing. The mechanism of such effective three-photon induced lasing is worth researching. Recently, spatial soliton also attracts great attentions. However, spatial soliton in liquid has not been reported.

In this letter, stable solitonlike filament is observed in solution, and the mechanism of high efficiency of three-photon induced lasing is revealed by analyzing the formation of the filament. Furthermore, the experimental and theoretical works in this letter will stimulate development of potential applications of high order optical nonlinearity.

In our experiment, we use a solution of heterocyclic molecules dissolved in dimethylsulphoxide, within which high efficiency lasing can be observed, as reported in the earlier letter.¹¹ The relevant parameters for the solution are $n_0=1.478$, $n_2=2.5 \times 10^{-3} \text{ cm}^2/\text{GW}$, $n_4=2.38 \times 10^{-4} \text{ cm}^4/\text{GW}^2$, and $\gamma=2.53 \times 10^{-2} \text{ cm}^3/\text{GW}^2$. n_0 is the refractive index, n_2 and n_4 are the linear refractive index, γ is three-photon absorption coefficients. The linear absorption peak wavelength of the solution is 474 nm and the emission peak wavelength is 610 nm. From 550 nm to 2 μm , there is negligible linear absorption. Our sample is a dye solution with concentration $d_0=0.02 \text{ mol}^{-1}$ in a 1 cm long quartz cell. The wavelength of the input laser is 1.3 μm , which is the three-photon absorption wavelength of the solution.

The experimental setup is shown in Fig. 1. The excitation source is a femtosecond laser train obtained from an optical parametric generator (Spectra Physics, Model: OPA-800C, USA). The pulse duration is 120 fs, and the repetition rate is 1 kHz. The infrared laser enters through a low-pass filter that cuts off the light of $\lambda < 800 \text{ nm}$, to screen out any spurious radiation at other wavelengths (originating from the OPA) that might affect the measurements. The intensity of

the laser beam is adjusted by the neutral density filters. The single pulse energy can be varied from 0 to 4 μJ . The laser beam with wavelength of 1.3 μm is focused into the sample cell via a lens of focal length $f=20 \text{ cm}$. We define the laser propagation direction to be along Z, and chose $Z=0$ to be the input surface of the cell, as shown in the inset of Fig. 1. The diameter of the 1.3 μm input laser beam is 500 μm at $Z=0$. In our experiment, we adjust the focus to $Z=6.3 \text{ mm}$ when the cell is empty, so when the cell is filled with solution, the focus is located at $Z=9 \text{ mm}$ (owing to the refractive index of the solution). The propagation of the infrared laser beams is observed through up-converted fluorescence of the dye collected by an optical microscope connecting to a charge coupled device (CCD) and a computer. We acquire images of the light propagating in the cell approximately every 0.5 mm.

In Fig. 1, at $Z=0$, the full diameter of the 1.3 μm laser beam is 500 μm . The outer (green) part of the beam in Fig. 1 shows the low density part of the beam, where the energy density is not high enough to induce three-photon absorption up-conversion fluorescence. This part cannot be observed by the CCD system (though it can be measured by an energy meter). The high-density center part of the laser beam (plotted in red) is where the energy density is high enough to induce observable three-photon absorption up-conversion fluorescence.

The results recorded by our microscope and CCD system show that the diameter of the red part at $Z=0$ is about 110 μm . The interesting effects occur in the region where Z

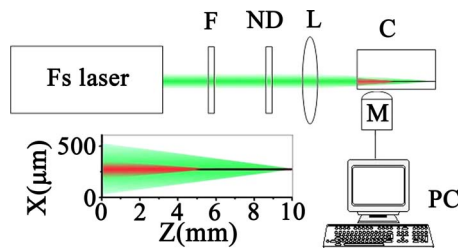


FIG. 1. (Color online) Experimental setup. F: filter; ND: neutral density filter; L: lens; C: cell filled with CQ medium; M: optical microscope connected with a CCD; and PC: personal computer. Inset: the magnified image of light propagation in solution.

^{a)}Author to whom correspondence should be addressed. Electronic mail: stswzhz@mail.sysu.edu.cn.

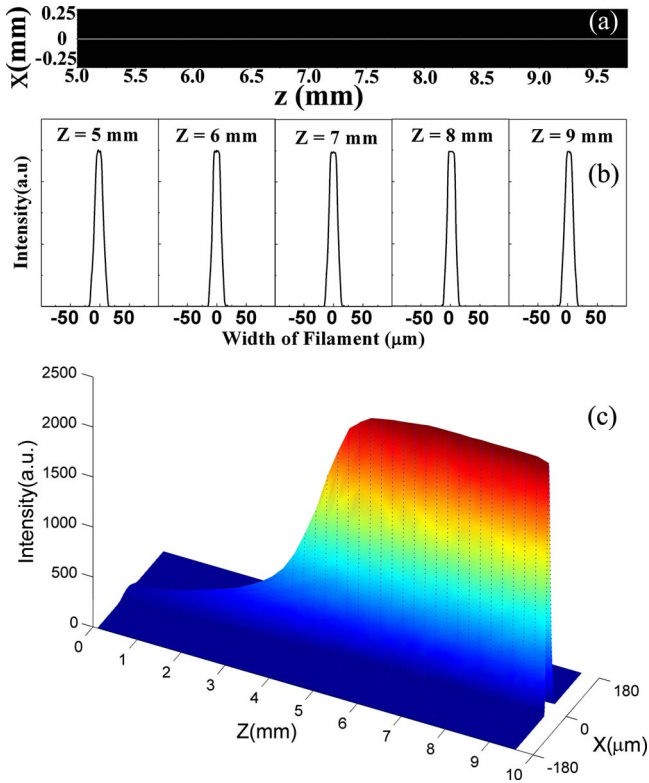


FIG. 2. (Color online) Experimental observation of stable soliton vs propagation distance. (a): the real image of the soliton (from 5 to 10 mm in the cell) that is taken by an optical microscope system in our experiment; (b): soliton profile evolves take from the real image (a), in which the width of filament is X in (a); (c): The three dimensional plot of up-converted fluorescent intensity distribution in the whole solution cell.

is between 5 mm to 10 mm. At low input power, fluorescence is hardly observed. When the input power reaches the threshold (where the intensity of the $1.3 \mu\text{m}$ laser beam is about 0.743 GW/cm^2), a stable filament appears. A single stable filament is observed when the intensity is from 0.743 to 2.97 GW/cm^2 . Figure 2 shows the results recorded by our microscope and CCD system at intensity of 2.12 GW/cm^2 . In Fig. 2, it is clearly to see that there is a stable solitonlike filament from $Z=5$ to 9.5 mm.

As the input light intensity is increasing, double or multiple filaments are observed. Each filament is stable and in steady shape. Besides laser intensity dependent experiments mentioned above, the wavelength-dependent, concentration-dependent experiments, and the solvent effect have been done. The stable spatial solitonlike filament only appears at high concentration solution, because only at high concentration solution quintic nonlinearity is high enough.

Simultaneous with the appearance of a stable solitonlike filament, the amplified spontaneous emission (ASE) induced by the fifth-order nonlinear optical process becomes surprisingly efficient. The efficiency reaches 2.04% at an input $1.3 \mu\text{m}$ laser intensity of 2.12 GW/cm^2 . Under the same experimental conditions (the same input laser intensity and the same experimental equipment, except that the input laser wavelength is $1 \mu\text{m}$), the efficiency of two-photon absorption induced ASE is 4.42%. This means that the existence of the stable solitonlike filament causes the lasing efficiency induced by three-photon absorption reaches the same order as that induced by two-photon absorption. As the input laser

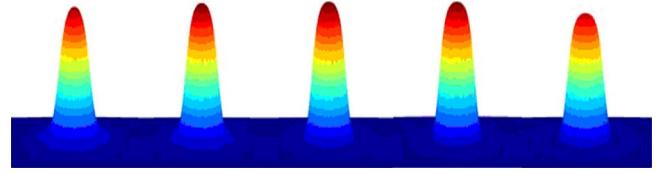


FIG. 3. (Color online) Numerical simulation based on Eq. (4). The five peaks according to $Z=5, 6, 7, 8,$ and 9 , similar to those in Fig. 2(b).

intensity increases, an even higher efficiency of three-photon absorption induced ASE is obtained.

To describe the spatial evolution of the light beam along the propagation coordinate z , we may write a modified cubic-quintic (CQ) model in a general rescaled form

$$i \frac{\partial \vec{E}(z)}{\partial z} + \frac{1}{2kn_0} \nabla_{\perp}^2 \vec{E}(z) + kn_2 |E(z)|^2 E(z) - kn_4 |E(z)|^4 E(z) = 0. \quad (1)$$

In this equation, n_2 and n_4 are positive constants determining the nonlinear response of the optical material with intensity I of the light beam.¹²

The multiphoton absorption processes can be described by the following phenomenological expression:¹³

$$\frac{dI(z)}{dz} = -\alpha I(z) - \beta I^2(z) - \gamma I^3(z) - \dots \quad (2)$$

Here, α , β , and γ are the one, two, and three-photon absorption coefficients of the medium. For our solution, there is no linear absorption ($\alpha=0$) at the frequency of the incident light. For a pure j -photon absorption process, Eq. (2) becomes

$$\frac{dI(z)}{dz} \propto -I^j(z). \quad (3)$$

Thus, considering three-photon absorption, Eq. (1) should include the fifth term that comes from Eqs. (2) and (3). So Eq. (1) becomes

$$i \frac{\partial \vec{E}(z)}{\partial z} + \frac{1}{2kn_0} \nabla_{\perp}^2 \vec{E}(z) + kn_2 |E(z)|^2 E(z) - kn_4 |E(z)|^4 E(z) + i\gamma |E(z)|^4 E(z) = 0. \quad (4)$$

In the Eqs. (1) and (4), the first term indicates the laser beam propagates along Z direction; the second term represents the diffraction of the beam. The third and fourth term characterizes self-focusing and self-defocusing, respectively. In the Eq. (4), the fifth term represents three-photon absorption.

A numerical simulation of the beam propagation is performed by using Eq. (4). The result is shown in Fig. 3. This plot is generated by extracting five transverse light-intensity profiles from the calculation. The evolution of the light-intensity profile shows the formation of a solitonlike filament.

For Z in the range of 5 to 9.5 mm in the cell, the light intensity reaches the threshold for dynamic equilibrium. Diffraction is overcome by the Kerr term (n_2). High density laser in the beam enhances the three-photon absorption drastically, which prevents the filament from collapsing tendency induced by the Kerr effect. Furthermore, part of the energy of infrared laser in the filament is absorbed by the solution

because of three photon absorption effect. But weak infrared laser outside the filament can compensate this energy loss owing to the focusing effect. There are similar cases in Refs. 14 and 15.

As the infrared laser propagates from $Z=5$ to 9.5 mm, the stable solitonlike filament appears, which makes the major part of pumping infrared laser be localized within the solitonlike filament. The localization of pumping infrared laser in stable solitonlike filament leads to the effective three photon absorption in the whole filament. The experimental results show that high efficiency of lasing induced by three-photon absorption is the result of stable solitonlike filament.

In conclusion, this work discovers that a stable spatial solitonlike filament can appear in solution with high quintic nonlinearity, which is the cause of effective three-photon induced lasing. The filament is the result of a stable mutual equilibrium among cubic nonlinearity, diffraction, and quintic nonlinearity. Furthermore, as well as revealing the mechanism of three-photon induced lasing, this work will make many practical applications of high order nonlinear optical processes possible.

This work is supported by the National Natural Science Foundation of China (Grant Nos. 10874250, 10674183, 50532030, and 20771001).

¹M. Göppert-Meyer, *Ann. Phys.* **9**, 273 (1931).

²W. Kaiser and C. G. B. Garret, *Phys. Rev. Lett.* **7**, 229 (1961).

³M. Albota, D. Beljonne, J. L. Brédas, J. E. Ehrlich, J. Y. Fu, A. A. Heikal, S. E. Hess, T. Kogej, M. D. Levin, S. R. Marder, D. McCord-Maughon, J. W. Perry, H. Rockel, M. Rumi, G. Subramaniam, W. W. Webb, X. L. Wu, and C. Xu, *Science* **281**, 1653 (1998).

⁴S. Kawata, H.-B. Sun, T. Tanaka, and K. Takada, *Nature (London)* **412**, 697 (2001).

⁵B. H. Cumpston, S. P. Ananthavel, S. Barlow, D. L. Dyer, J. E. Ehrlich, L. L. Erskine, A. A. Heikal, S. M. Kuebler, I. S. Lee, D. McCord-Maughon, J. Qin, H. Röckel, M. Rumi, X. Wu, S. R. Marder, and J. W. Perry, *Nature (London)* **398**, 51 (1999).

⁶W. Denk, J. H. Strickler, and W. W. Webb, *Science* **248**, 73 (1990).

⁷J. B. Ehrlich, X. L. Wu, I. S. Lee, Z. Y. Hu, H. Röckel, S. R. Marder, and J. W. Perry, *Opt. Lett.* **22**, 1843 (1997).

⁸C. F. Zhao, G. S. He, J. D. Bhawalkar, C. K. Park, and P. N. Prasad, *Chem. Mater.* **7**, 1979 (1995).

⁹H. Z. Wang, X. G. Zheng, W. D. Mao, Z. X. Yu, and Z. L. Gao, *Appl. Phys. Lett.* **66**, 2777 (1995).

¹⁰G. S. He, P. P. Markowicz, T.-C. Lin, and P. N. Prasad, *Nature (London)* **415**, 767 (2002).

¹¹H. H. Fan, K. S. Wu, H. Z. Wang, Y. P. Tian, G. L. Law, K. L. Wong, and W. T. Wong, *Chem. Phys. Lett.* **449**, 77 (2007).

¹²C. L. Zhan, D. Q. Zhang, D. B. Zhu, D. Y. Wang, Y. J. Li, D. H. Li, Z. Z. Lu, L. Z. Zhao, and Y. X. Nie, *J. Opt. Soc. Am. B* **19**, 369 (2002).

¹³G. S. He and S. H. Liu, *Physics of Nonlinear Optics* (World Scientific, Singapore, 2000).

¹⁴E. M. Wright, B. L. Lawrence, W. Torruellas, and G. Stegeman, *Opt. Lett.* **20**, 2481 (1995).

¹⁵B. L. Lawrence and G. I. Stegeman, *Opt. Lett.* **23**, 591 (1998).